tions, exhibit significantly enhanced *in vitro* activities with corresponding Ki values in the range of tenths of pM to several nM. The structure-activity relationship (SAR) observed within a small library of ca. 60 substituted carboranes and metallacarboranes is discussed.

These results are complemented by synchrotron structures of enzyme-inhibitor complexes and by a short overview of pharmacologically relevant factors such as plasma protein binding, cell membrane penetration, and basic results from toxicology and pharmacokinetic studies (mouse model) performed on a panel of the selected inhibitors of CA IX enzymes. Due to promising inhibitory properties, these compounds are thus primarily considered as candidates for drugs applicable in cancer treatment.

1. J. Brynda, P. Mader, V. Šícha, M. Fábry, K. Poncová, M. Bakardiev, B. Grüner, P. Cígler, P. Řezáčová, *Angew. Chem., Intl. Ed. Eng.*, 2013, *52*, 13760.

Supported by Czech Science Foundation, Project No. 15-05677S and in part by Technology Agency of the Czech Republic, Project No. TE01020028 (pharmacology and in vivo testing). Also support from institutional research projects RVO 68378050, 61388963, and 61388980 by the Academy of Sciences of the Czech Republic is appreciated.

Session III, Tuesday, September 13

L6

NMR AND X-RAYS ARE NOT ENEMIES ANYMORE

Pavel Srb

Ústav organické chemie a biochemie AV ČR, v. v. i, Flemingovo nám. 2, Praha 6

NMR spectroscopy and X-ray crystallography have traditionally been viewed as rivals in three dimensional protein structure elucidation, NMR being less successfull one. The fundamental difference between NMR and X-rays lies is the following: X-rays provides almost direct spatial information about atomic positions, while NMR signal directly encodes frequency of nuclei (more precisely of nuclear spins). After introducing basic physical principles of NMR, the standard pipeline of sample preparation and signal assignment will be explained, with emphasis on description to various useful paramaters that can be extracted without previous structure knowledge, however are very useful in characterizaation of a system under scope. Namely chemical shifts, residual dipolar couplings and paramagnetic relaxation enhancemets. A special attention will be paid to NMR methods for characterization of protein dynamics on various timescales. Specifically the possibility of characterizing the low populated conformational protein states opens a path to a challenging goal of describing protein as a dynamic ensemble of functional states. A real life examples of studies of protein-protein and protein-small molecule interactions will be described and explained.

L7

POZITRONOVÁ ANIHILAČNÍ SPEKTROSKOPIE

Jakub Čížek

Katedra fyziky nízkých teplot, Matematicko-fyzikální fakulta Univerzity Karlovy v Praze

Pozitronová anihilační spektroskopie využívá pozitron jako sondu ke studiu struktury materiálu. V pevných látkách jsou pozitrony anihilovány elektrony a emitované anihilační záření přináší informaci o parametrech anihilačního procesu. Hlavní pozorovatelné jsou doba života pozitronu a Doppleruv posuv energie anihilačních fotonů. Pozitron implantovaný do dokonalého krystalu je delokalizovaný v krystalové mříži a pozitronová hustota má formu modulované rovinné vlny. Defekty krystalické mříže spojené s volným objemem (např. vakance, dislokace, hranice zrn atd.) představují pro pozitron potenciálové jámy a mohou vést k záchytu pozitronu, tj. muže dojít ke vzniku vázaného stavu pozitronu v defektu. Takto zachycené pozitrony mají delší dobu života než pozitrony delokalizované v krystalické mríži. Doba života pozitronu je určena lokální elektronovou hustotou v místě defektu. Každý stav pozitronu v daném materiálu přispívá do spektra dob života pozitronu exponenciální komponentou. Změřením dob života těchto exponenciálních komponent je možné identifikovat typy defektu ve studovaném materiálu. Z intenzit techto komponent lze potom pomocí vhodného modelu určit koncentrace defektu.

V přednášce bude vysvětlen princip pozitronové anihilační spektroskopie a ilustrovány její možnosti na příkladě studia ultra jemnozrnných materiálů připravených silnou plastickou deformací. Budou rovněž zmíněny oblasti kdy se informace získaná pomocí pozitronové anihilacní spektroskopie překrývá s informací o reálné struktuře materiálu získané studiem tvaru rozšíření difrakčních profilů rtg. záření.

L8

NON-TRADITIONAL APPLICATIONS OF THE MÖSSBAUER SPECTROSCOPY

A. Lančok

Institute of Inorganic Chemistry of the CAS, Husinec-Řež č.p. 1001, 250 68 Řež, Czech Republic
ada@iic.cas.cz

Nanomaterial is interesting material for artworks, biomedical and industrial applications especially in the field of nuclear installations. Our aim was to study of iron-containing nanoparticles in different type of materials (see Fig. 1); e.g. disks [1], powders [1-3], thin films etc. The methods for preparing of nanomaterials have attracted considerable scientific interest in recent years. These materials are structurally well ordered with very well-defined and exhibit unique physical and chemical properties determined by their practically applications. The aim of the lecture is to give an overview of current trends and perspectives in the research of above mentioned classes of nanomaterials.

Mössbauer spectrometry of the biological tissues confirms the presence of hematite, ferrihydrite and maghemite/magnetite in ferritin derived from human spleen and brain tissues. The minerals are present in a form of small (about 4-5 nm in size) grains with highly disordered structure. At room temperature all agglomerates of ferritin nanoparticles show non-magnetic behaviour. Employing Mössbauer effect measurements, the latter was determined to be of 16 K for the human spleen. Fig. 2 shows the evolution of Mössbauer spectra of low temperature dependencies.

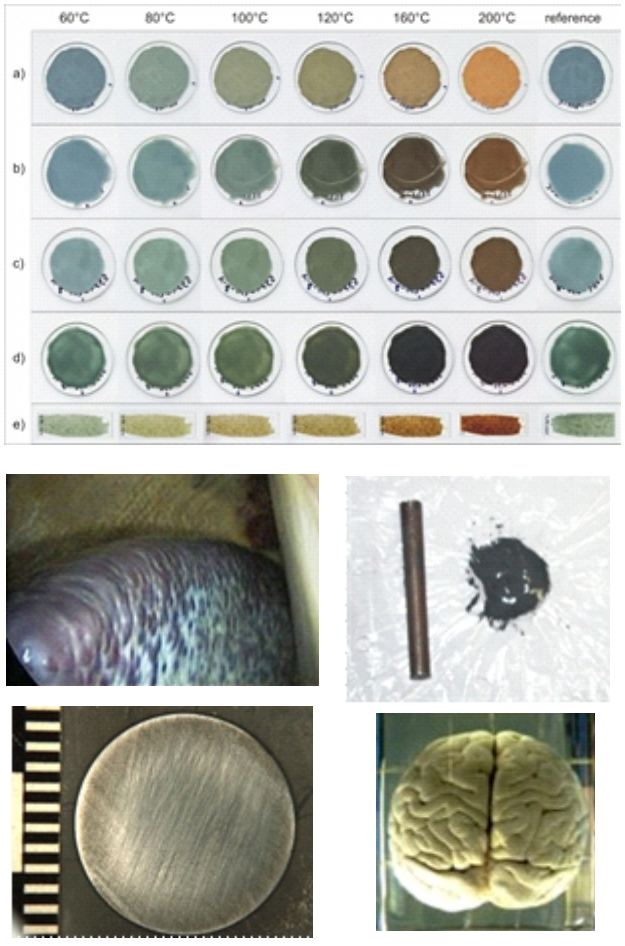

Figure 1. Different type of nanomaterials.

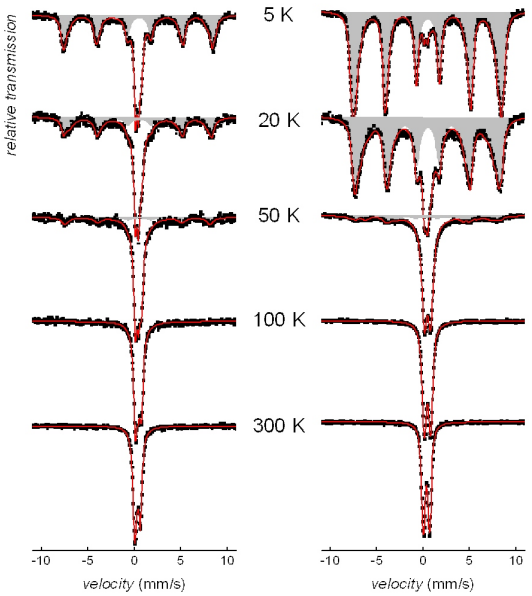

Figure 2. Temperature dependences.

A study of pure synthetic (as well as partly oxidised) vivianite (materials for artworks) covering the whole extent of the temperature-related stability of its structure is being published for the first time in [2]. The results show that already temperatures around 70 °C are damaging to vivianite, therefore, some of the recommended procedures during vivianite's synthesis including digestion under increased temperatures should be avoided. Mössbauer spectra demonstrated that the temperature-induced oxidation of vivianite starts at 90°C, which corresponds with the increase of the amount of metavivianite. Fig. 3 shows the evolution of Mössbauer spectra of vivianite with increasing temperature, and illustrates the amounts of Fe^{2+} and Fe^{3+} after each heating step.

The transmission Mössbauer spectra of the powder and bulk samples show clear six-line pattern with only traces of a central single absorption line (shown in blue component in its central part). The six-line patterns in both spectra are assigned to magnetically ordered ferrite phase. They were fitted by 6 sextets. S1 through S5 represent those Fe atoms that have n Cr in their nearest shell with n = 0 up to 4. The sextet S6 with the lowest hyperfine field comes from the unresolved contribution of Fe atoms with 5 and more Cr nearest neighbours. Decomposition of the sextuplet part of

spectra to components is plotted in Fig.4 in different shades of grey colour.

Mössbauer spectrometry was chosen as a principal method of investigation. Complex behaviour of magnetic and non-magnetic phases of nanomaterials was identified in the samples by Conversion Electron Mössbauer Spectrometry and transmission technique. Structural arrangement was studied by electron microscopy with energy dispersive spectrometry, X-ray diffraction, etc. In the presentation, I will discuss the properties of different type of nanomaterials for various applications

1. A. Lancok, T. Kmjec, M. Stefanik, L. Sklenka, M. Miglierini , *Croatia Chemica Acta*, **88**, (2015), 355.
2. Z. Cermakova, S. Svarcova, J. Hradilova, P. Bezdicka, A. Lancok, V. Vasutova, J. Blazek, D. Hradil, *Spectrochimica Acta Part A-Molecular and Biomolecular Spectroscopy*, **140**, (2015), 101.
3. M. Miglierini, A. Lancok, *Acta Phys. Polonica A*, 118, (2010), 944.

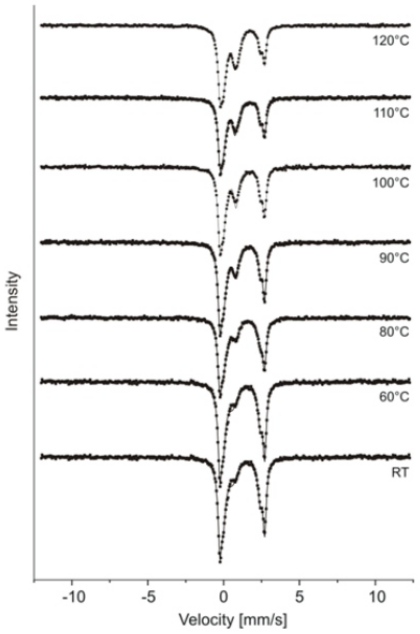

Figure 3. Mössbauer spectra of ground natural vivianite crystals used for the model samples after exposition to a series of heating steps [2].

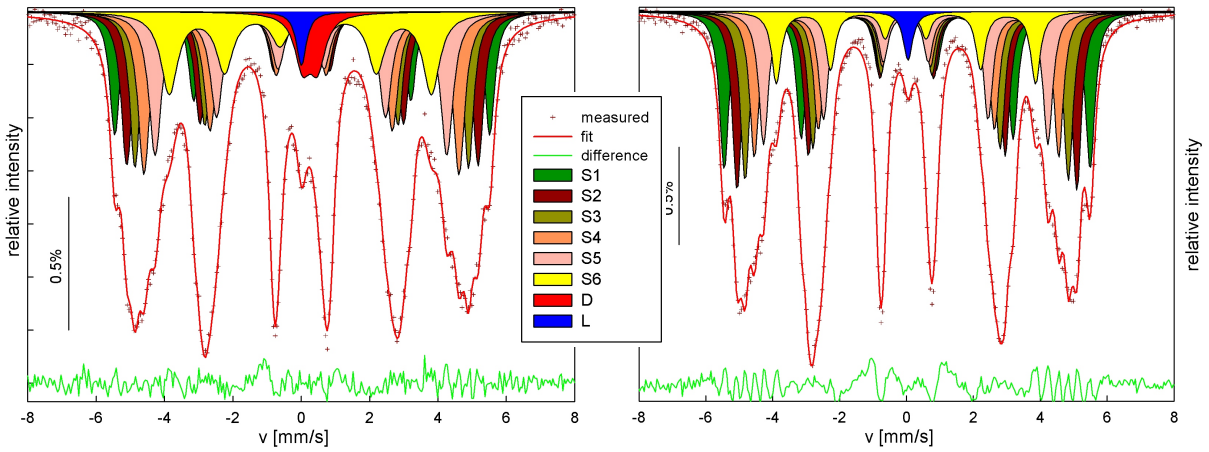

Figure 4. The decomposition of transmission Mössbauer spectra of the sample: (a) powder from of the surface of the disk and (b) bulk sample (transmission spectrum of the foil prepared from the disk).

L9

METHODS AND TOOLS FOR ANALYSIS OF NANOMATERIALS BY MEANS OF ATOMIC PAIR DISTRIBUTION FUNCTION

Z. Matěj[1,2], M. Dopita[2], M. Paukov[2], L. Havela[2]

[1]MAX IV Laboratory, Lund University, Lund, Sweden
[2]Faculty of Mathematics and Physics, Charles University in Prague, Praha, Czech Republic
zdenek.matej@maxiv.lu.se

Atomic Pair Distribution Function (PDF) describes distances between pairs of atoms in the matter on a nano-scale. A radial PDF weighted by atomic scattering factors can be obtained by means of X-ray and neutron total scattering on powder, nanocrystalline, amorphous or liquid samples. Beside Bragg intensity analysed by classical powder diffraction PDF brings information on a short range order from the diffuse scattering component. The number of scientific problems resolved by this method is rapidly growing thanks to multiple factors: as improved availability of dedicated neutron instruments, developments in X-ray detectors and laboratory instruments but also because of an

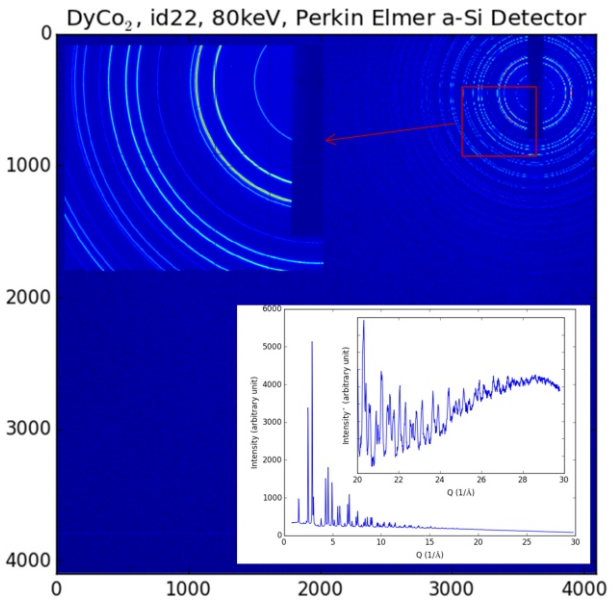

Figure 1. High energy synchrotron data from a temperature calibration sample of $DyCo_2$. The inset shows image data reduced to a powder pattern using `pyFAI`.

advent of software and methods for straightforward PDF retrieval, modelling and analysis.

In this presentation we give a brief overview of the method and handy tools for PDF analysis. This is illustrated on an application case of X-ray data from nanocrystalline alloyed Uranium hydrides. We show some basic thoughts one shall do before starting a PDF experiment, list of some noticeable neutron instruments, demonstrate several tools for X-ray data reduction (see an example received from `pyFAI` [1] in Fig. 1 or `srx-planar` [2]) and a procedure to obtain the experimental PDF by means of `PDFgetX3` [3]. We mention several tools for PDF simulations (DISCUS [4]) and data fitting (`DiffPy` suite [5]) that we considered very useful for working with nanocrystalline materials.

Our scientific problems is concerning U-hydrides. For us they present a probe to study an impact of expansion of the U lattice, allowing formation of U moments and their ferromagnetic ordering. Starting from (bcc) -U alloys using doping with Zr or Mo, different varieties of UH_3 were synthtised [6]. Whereas Zr-dopping resulted in a fomation of (20 nm) nanocrystallites with -UH_3 cubic structure, pure Mo-alloyed UH_3 is almost amorphous corresponding to very purely (1 nm) nanocrystalline material with -UH_3 like structure [7] (Fig. 2). Despite of these structural differences both types of hydrides behave similarly as ferromagnets with Curie temperature T_C 170–200 K [6]. A striking phenomena observed in UH_3 alloys is a large volume magnetostriction. This we tested in low temperature experiments.

Analysis of real powder samples can be a complex problem especially if instrumental effects can influence the results and as the structure of the sample is often not ideal, e.g. becouse of presence of multiple phases or impurities. This is why beside fitting of PDF data with a structural model we employ alternative menthods of fitting of individual PDF maxima with phenomenological functions (a parSCAPE software can be useful for this [8]). Finally X-ray data analysis is complemented with preliminary neutron scattering simulations.

1. G. Ashiotis, A. Deschildre, Z. Nawaz, J.P. Wright, D. Karkoulis, F.E. Picca, J. Kieffer, *J. Appl. Cryst.*, **48**, (2015), 510. doi: 10.1107/S1600576715004306.
2. X. Yang, P. Juhás, S.J.L. Billinge, *J. Appl. Cryst.*, **47**, (2014), 1273. doi: 10.1107/S1600576714010516.
3. P. Juhás, T. Davis, C.L. Farrow, S.J.L. Billinge, *J. Appl. Cryst.*, **46**, (2013), 550. doi: 10.1107/S0021889813005190
4. Th. Proffen and R.B. Neder, *J. Appl. Cryst.*, **30**, (1997), 171. doi: 10.1107/S002188989600934X
5. P. Juhas, C.L. Farrow, J. Liu, W. Zhou, P. Tian, Y. Shang, S.J.L. Billinge, Acta *Cryst.*, **A67**, (2011), C143. doi: 10.1107/S0108767311096498
6. I. Tkach, M. Paukov, D. Drozdenko, M. Cieslar, B. Vondráčková, Z. Matěj, D. Kriegner, A.V. Andreev, N.-T.H. Kim-Ngan, I. Turek, M. Diviš, L. Havela, *Phys. Rev. B*, **91**, (2015), 115116. doi: 10.1103/PhysRevB.91.115116
7. L. Havela, M. Paukov, I. Tkach, V. Buturlim, Z. Matej, S. Maskova, I. Turek, M. Divis, D. Drozdenko, M. Cieslar, M. Dopita, Z. Molcanova, M. Mihalik, *MRS Advances*, (2016). doi: 10.1557/adv.2016.287
8. L. Granlund, S.J.L. Billinge, P.M. Duxbury, Acta *Cryst.*, **A71**, (2015), 392. doi: 10.1107/S2053273315005276

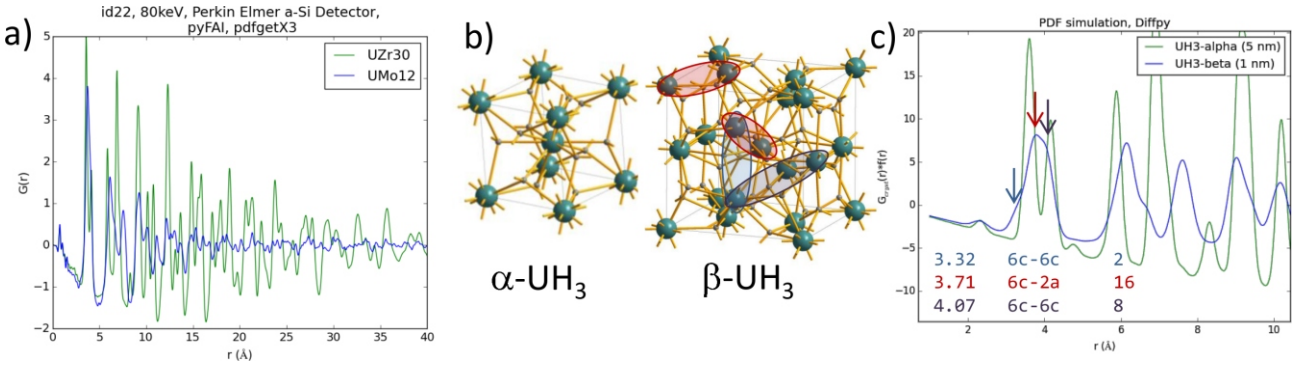

Figure 2. (a) comparison of experimental PDF of $(UH_3)_{0.70}Zr_{0.30}$ and $(UH_3)_{0.88}Mo_{0.12}$, (b) unit cell structures of -UH_3 and -UH_3, (c) `DiffPy` PDF simulations with marked 3 closest U-U distances in UH_3.

SL2

STRUCTURE ANALYSIS OF NANOFIBERS PREPARED BY NANOSPIDER TECHNOLOGY

P. Ryšánek[1], P. Čapková[1], M. Munzarová[2], A. Čajka[1], M. Barchuk[1]

[1]Faculty of Science, J. E. Purkyně University, České mládeže 8, 400 96 Ústí nad Labem
[2]Nanovia, s. r. o., Litvínov, Podkrušnohorská 271, 436 03 Litvínov – Chudeřín

Polymer nanofibers are used in wide range of activities in everyday life, such as: filtration [1], protective closing, pharmaceuticals [2], etc. The greatest attention is paid on nanofibers, that have great biocompatibility. These nanofibers can be used as wound covers in biomedicine. The first representative is nylon 6, which has very good biocompatibility and also very good mechanical properties [3]. The other representative is chitosan, which is polysacharide, and due to its origin it has also very good biocompatibility. Chitosan itself have also antibacterial properties [4, 5].

The structure of nylon 6 and chitosan was studied by many authors [6 - 9], but the structure of these nanofibers prepared by NANOSPIDER technology is less studied [10, 11], although this technology is widely used in industry and due to is the knowledge of the structure very important, because the structure has significant influence on nanofiber properties.

Nylon 6

Structure of nylon 6 polymer is very well known. It was resolved that nylon 6 is polymorphic and has two crystal structures: alpha form which was described by Brill [12] and Holmes [13] and gamma form which was determined by Holmes [13]. Both structures are monoclinic and differ from each other by density and arrangement of polymeric chains. The arrangement of the polymeric chains can be seen on Figure 1.

It is known that the electrospinning preparation of nylon 6 nanofibers leads to three structural phases: alpha, gamma and amorphous phase of nylon 6. The dependence of nylon 6 structure on the NANOSPIDER arrangement was invetsigated. It has been determined, that the phase composition of nylon 6 nanofibers (i.e. the content of alpha, gama and amorphous phase) depends on electrode distance. In our previous work the core-shell structure model has been suggested, based on combination of XRD and XPS measurements [10]. The fibers exhibit also very strong texture in direction (010). The typical XRD pattern of nylon 6 nanotextile is on Figure 2.

Chitosan

It is difficult to prepare pure chitosan nanotextiles using electrospinning [8]. Therefore it is often used the mixture of chitosan with other polymers [14, 15]. For easier electrospinning we used mixture of chitosan and polyethylene oxide (PEO). For further applications in medicine the mixture of chitosan, PEO and gelatin has been used. The nanotextile was also cross-linked at 130°C. The research was aimed in order to investigate the effect of gelatin and cross-linking on the nanotextile structure and properties. It has been found, that:

- The presence of gelatin has strong effect on nanofiber structure, as it prevents the crystallization of chitosan.
- After the thermal crosslinking the gelatin climbs to surface of the fibers and reduces the porosity of the nano-textile.
- The thermal crosslinking itself (without gelatin) also disrupts the structure of nanofibers and reduces the crystallinity of chitosan and PEO.

1. H. R. Ant, M. P. Bajgai, Ch. Yi, R. Nirmala, K. T. Nam, W. Baek, H. Y. Kim., *Colloids and Sur faces A: Physicochemical and Enginering Aspects*. 370 (2010) 87-94.

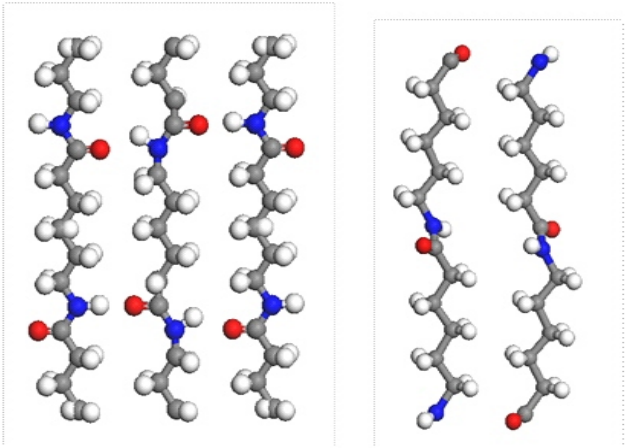

Figure 1. Arrangement of polymer chains of nylon 6 in ab plane in crystal structure of alpha phase (left) and gamma phase (right).

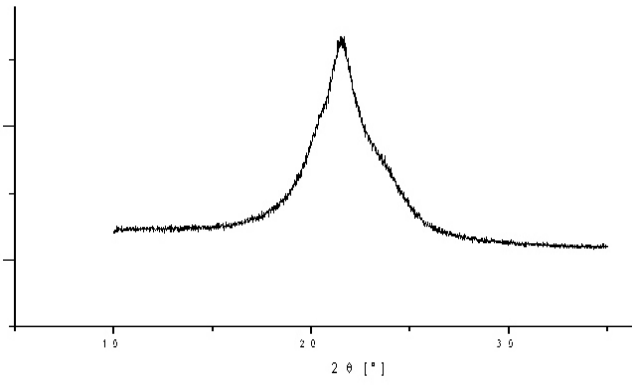

Figure 2. Typical XRD profile of nylon 6 nanotextile.

2. P. Raghavan, X. Zhao, J. K. Kim, J. Manuel, G. S. Chauhan, J. H. Ahn, C. Nan, *Electrochim. Acta* 54 (2008), 228-234.

3. J. L. Pey, *Anti_Corros Methods Matter* 44, (1997), 94-99.

4. F-L. Mi, Y-C. Tan, H-F. Liang, H-S. Sung, *Biomaterials* 23 (2002), 181–191.

5. I. Leceta, P. Guerrero, I. Ibarburu, M.T. Duenas, K. de la Caba, *J. Food Engineering* 116 (2013), 889-899.

6. S. Zhang, W. S. Shim, J. Kim, *Materials* 30 (2009), 3659-3666.

7. S. S. A. Deyah, M. H. E. Newehy, R. Nimala, A. A. Megeed, H. Y. Kim, *Korean Journal of Chemical Engineering* 30 (2013), 422-428.

8. S.D. Vrieze, P. Westbroeak, T.V. Camp, L. van Langenhove, *J. of Materials Sc.* 42 (2007), 8029–8034.

9. K. Ohkawa, K-I. Minato, G. Kumagai, S. Hayashi, H. Yamamoto, *Biomacromolecules* 7 (2006), 3291–3294.

10. P. Čapková, A. Čajka, Z. Kolská, M. Kormunda, J. Pavlík, M. Munzarová, M. Dopita, D. Rafaja, *J. Polym. Res.* 22 (2015), 101.

11. M. Barchuk, P. Čapková, Z. Kolská, J. Matoušek, D. Poustka, L. Šplíchalová, O. Benada, M. Munzarová, *J. Polym. Res.* 23 (2016), 19-25.

12. R. Brill, *Z. Physik. Chem* B 53 (1943), 61-66.

13. R. Holmes, C. W. Burn, D. L. Smith, *J. Polym. Sci.* 17 (1955), 619-624.

14. M. Spasova, N. Manolova, D. Paneva, I. Rashkov, *e-Polymers* 56 (2004), 1–12.

15. K. Ohkawa, T. Kitagawa, H. Yamamoto, *Macromolecular Materials and Engineering* 289 (1) (2004), 33–40.

The authors acknowledge the assistance provided by the Research Infrastructure NanoEnviCz, supported by the Ministry of Education, Youth and Sports of the Czech Republic under Project No. LM2015073.

SL3

INTERACTION OF NYLON 6 WITH ANTIBACTERIAL MOLECULES

Iryna Gren, Marek Malý, Pavla Čapková

Faculty of Science, Jan Evangelista Purkyně University in Ústí nad Labem, Česká mládeže 8, 40096 Ústí nad Labem

In connection with the development of technologies for production and use of nanomaterials, which are due to particular physical, chemical, biological, pharmacological and mechanical properties are able to cause unpredictable effects on biological objects in modern science there is a problem ethical use of nano substances and their risk assessment for the body humans and the environment. Although studies the effects of certain nanostructures performed very active, there are difficulties in forecasting migration and interaction of nanoparticles.

Nylon 6 is a linear addition polymer of caprolactam. This means, that the nylon 6 can be seen as the product of intramolecular interactions carboxyl group and 6 -amino-caproic acid [1, 2]. Upon cooling nylon-6 from the melt, a semicrystalline structure is obtained, which is characterized by polymorphism. There are two crystalline phases and (see Fig. 1) [3, 4, 5]. They differ in arrangement of chains and network of hydrogen bonds. Interaction of nylon 6 with antibacterial molecules is interesting for the design of antibacterial nanofiber filters [6]. To model these interactions we used molecular modeling using empirical force field in Materials Studio modeling environment.

Three types of antibacterial molecules have been used in the present study: chlorhexidine, BTAB (benzyltrimethyl amonium bromide), DTAB (dodecyltrimethyl amonium bromide) [7]. Interaction energy, which defines the stability of the complex nylon6-antibacterial molecule has been calculated and compared for each individual antibacterial substance [8].

The preferable orientation of molecules on the nylon6 surface, represented by crystalline phase, was studied for very low and realistic surface density of all 3 antibacterial ligands.

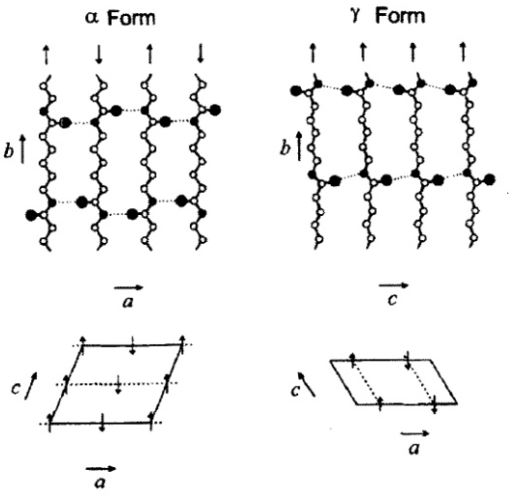

Figure 1. Structures of the and forms of nylon-6

The authors acknowledge the assistance provided by the Research Infrastructure NanoEnviCz, supported by the Ministry of Education, Youth and Sports of the Czech Republic under Project No. LM2015073.

1. Arimoto, H., Ishibashi, M., and Hirai, H., *Crystal Structure of the form of Nylon 6*, *J. Polym. Sci. A* **3**, 317-326 (1965).

2. Shenoy S.L, Bates W.D, Frisch H.L, Wnek G.E (2005), *Role of chain entanglements on fiber formation during electrospinning of polymer solutions: good solvent, non-specific polymer-polymer interaction limit*, Polymer 46:3372.

3. Siddharth Dasgupta, Wills B. Hammond, and William A.Goddard III, *Crystal Structures and Properties of Nylon Polymers from Theory*, Received December 22, 1994.¨Revised Manuscript Received July 19, 1996.

4. N.S. Murthy, R.G. Bray, S.T. Correale, R.A.F. *Moore Drawing and annealing of nylon-6 fibres: studies of crystal growth, orientation of amorphous and crystalline domains and their influence on properties,* Polymer, 36 (20) (1995), pp. 3863–3873.

5. Yi Liu, Li Cui, Fangxiao Guan, Yi Gao, Nyle E. Hedin, Lei Zhu,*, and Hao Fong† *Crystalline Morphology and Polymorphic Phase Transitions in Electrospun Nylon 6 Nanofibers*, *Macromolecules*. 2007 ; 40(17): 6283–6290.

6. Pavla Čapková*, Antonín Čajka, Zdenka Kolská, Martin Kormunda, Jaroslav Pavlík, Marcela Munzarová, Milan Dopita, David Rafaja*, Phase composition and surface properties of nylon-6 nanofibers prepared by nanospider technology by various electrode distances,* Article in journal of Polymer Research 22(6), June 2015.¨

7. Veggeland, Kirsti; Nilsson, Svante. *Polymer-Surfactant Interactions Studied by Phase Behavior, GPC and NMR,* Langmuir (1995), 11 (6), 1885-92.

8. Shailesh M. Kolhe,Ashok Kumar, *Radiation-induced grafting of vinyl benzyl trimethyl ammonium chloride onto nylon-6 fabric*, Radiation Processing Group, 14 July 2006.